Marine Chemistry xxx (xxxx) xxx–xxx

Contents lists available at ScienceDirect

Marine Chemistry

journal homepage: www.elsevier.com/locate/marchem

Forms and distribution of Ce in a ferromanganese nodule

Matthew A. Marcus[a,*], Brandy M. Toner[b], Yoshio Takahashi[c]

[a] Advanced Light Source, Lawrence Berkeley National Laboratory, Berkeley, CA 94720, USA
[b] Department of Soil, Water, and Climate, University of Minnesota, St. Paul, MN 55108, USA
[c] Department of Earth and Planetary Science, Graduate School of Science, The University of Tokyo, Hongo, Bunkyo-ku, Tokyo 113-0033, Japan

ARTICLE INFO

Keywords:
Ferromanganese nodule
Cerium
X-ray spectroscopy
Chemical speciation

ABSTRACT

We studied the distribution and speciation of Ce in a previously-characterized ferromanganese nodule from the South Pacific Gyre using X-ray microspectroscopy.We find Ce in three types of environment – diffusely in all parts of the nodule except the Fe-rich, Mn-poor "matrix", fluorapatite grains with a negative Ce anomaly suggestive of an authigenic origin, and localized spots whose composition is consistent with a pseudobinary mixture of sorbed Ce^{4+} and a mix of sorbed Ce^{3+} and CeO_2. In contrast with some other elements such as Ti, there is no clear correlation of the Ce concentration in the diffuse areas with either that of Mn, Fe or any linear combination of the two.We argue that the CeO_2 came from oxidation of Ce^{3+} in the water column, while the Ce in the Mn-rich regions may have been initially deposited as Ce^{4+} and then partially reduced.

1. Introduction

Rare-earth elements (REE) have drawn much attention from geochemists not only for their economic utility but also for their usefulness in tracing the formation and subsequent evolution of many kinds of rocks and minerals.Among the REE, those which commonly exhibit two or more valence states are particularly interesting because they respond to redox conditions during and after deposition.In particular, Ce is famous for "Ce anomalies", in which its elemental abundance in a particular system is either greater or less expected based on the abundances of other REE (De Baar et al., 1991; Elderfield et al., 1988). These anomalies are, in part, due to the fact that Ce^{3+} can be oxidized to the less-soluble Ce^{4+}.

Ferromanganese nodules are slow-growing, layered mineral deposits with concentric growth patterns which may hold time-resolved records of geochemical conditions over many millions of years (Calvert and Cronan, 1978; Koschinsky and Hein, 2003). These materials contain a number of elements of geochemical interest such as Fe and Mn (major elements), and Cu, Ni, REE, Ti, and V (trace elements) (Bau et al., 2014; Hein et al., 2013; Peacock and Sherman, 2007; Takahashi et al., 2007). Using modern micro-analytical techniques, it is possible to study the abundances and speciation of these elements within specific zones of mineral accumulation (Manceau et al., 2002; Marcus et al., 2015; Marcus et al., 2004).Greater spatial resolution provides effectively greater time resolution, as well as insights into spatial-correlation between trace element speciation and specific mineral phases.If coupled to isotopic age-dating methods and trace element isotope fractionation observations, then a micro-analytical approach can provide the timing of mineral precipitation events, the chemical speciation and isotope signatures of trace element(s) sequestered in those conditions, at least if there has been no diagenetic changes or secondary re-deposition.While micro X-ray absorption spectroscopy cannot be used for trace elements present in concentrations as low as are accessible with some other methods, it does provide speciation and valence data.This method can thus be a useful addition to the suite of analytic methods employed in geochemical studies.While it is currently unusual to obtain all three analytical perspectives for ferromanganese nodules in a single study, the utility of using of two of the three approaches together has been demonstrated for marine mineral deposits (Marcus et al., 2015; Toner et al., 2016).

In a previous paper, we described in detail the growth rate (^{10}Be), mineralogy and stable isotope composition of the major element Fe, and speciation of trace elements Ti and V for a hydrogenetic ferromanganese nodule from the South Pacific Gyre (Marcus et al., 2015). In this manuscript, we return to that nodule and concentrate on the speciation and spatial distribution of Ce.We find that, although the nodule grew in an oxic environment and is mostly composed of oxidized forms of Fe^{3+} and Mn^{4+}, it contains Ce in the reduced, 3+ state as well as sorbed Ce^{4+} and $Ce^{4+}O_2$.Further, the distribution of Ce breaks down into three patterns, each characterized by differing speciation.We find mixed Ce^{3+}/Ce^{4+} disseminated throughout most of the nodule, CeO_2-rich spots, and apatite ($Ca_5(PO_4)_3X$, X = F, Cl, OH) crystals containing Ce^{3+} and Ce^{4+}.These observations are surprising in the light of previous work on Ce in ferromanganese nodules in which only Ce^{4+} was

* Corresponding author.
E-mail address: mamarcus@lbl.gov (M.A. Marcus).

https://doi.org/10.1016/j.marchem.2018.03.005
Received 1 September 2017; Received in revised form 19 March 2018; Accepted 22 March 2018
0304-4203/ Published by Elsevier B.V.

found (Takahashi et al., 2007; Takahashi et al., 2002). In that previous work, it was suggested that the Ce either sorbed onto Mn, a process which they showed was accompanied by oxidation of Ce^{3+} to Ce^{4+} or adhesion of Ce^{4+}-bearing particles, presumably CeO_2.However, their work was done with a "macro" (~1 mm) beam.We show that the use of a micro beam reveals much more complexity than had been previously found.We will describe the nodule and our findings regarding Ce and suggest some interpretations of what we find.

2. Nodule description and methods

Since the nodule was described in (Marcus et al., 2015), we will only summarize its provenance and basic properties here.The nodule came from a site, South Pacific Gyre-2, at 26°03.090′S, 156°53.650′W, at 5126 m water depth.This site is located in a region of abyssal hill topography, with several small seamounts scattered about the region.The coring site is located within magnetic polarity Chron 34n, so the crustal age may range from 84 to 124.6 Ma (Gradstein and Ogg, 2002). Based on a tectonic reconstruction of the region (Larson et al., 2002), the crust was accreted along the Pacific-Phoenix spreading center ~95 Ma ago at ultra-fast spreading rates (~90 km/Ma, half-rate).The water column overlying the site is one known to be of low primary productivity.

A polished petrographic thin section of the nodule was prepared by Spectrum Petrographics, Inc. The nodule was embedded in 3 M Scotchcast #3, mounted on a fused silica slide with Loctite Impruv 363 adhesive, and sectioned to a 30 µm slice with a diamond-polished electron-microprobe finish.$^{10}Be/^{9}Be$ analysis was used to derive a growth rate of (3.8–4.2) ± 0.7 mm/Ma.

Following the notation of (Marcus et al., 2015), we define "inner" and "outer" regions of the nodule which show differing morphology and Fe/Mn ratios.The "inner" zone contains the oldest material, while the "outer" is close to the surface and more recently deposited.While both zones show botryoidal morphologies with an Fe-rich, Mn-poor "matrix" between botryoids, the inner zone is conspicuously richer in matrix and has a higher Fe/Mn ratio in the botryoids than the outer zone.

X-ray fluorescence (XRF) maps and XANES (X-ray absorption near-edge structure) spectroscopy were done on Beamline 10.3.2 at the Advanced Light Source.The pixel size of the maps ranged from 7 to 20 µm.In order to understand the patterns of occurrence of Ce species, we performed chemical-state mapping by doing XRF at energies of 5715.0, 5725.5, 5728.35, 5731.5 and 5746.0 eV and a pixel size of 7 µm.In order to reduce any effects of sample drift during mapping, we took the maps in such a way that each scan line was taken at each energy before moving to the next line.This mode is in contrast with the older procedure of taking the whole map at one energy, then taking it again at the next, etc.The lowest-energy maps were used to image the distributions of Ti, Ca and, for some regions, Cl.Additional maps were taken on the same areas at 10 keV, in order to see the distributions of Mn, Fe, Ni and Cu.These maps were taken separately from the chemical-state maps because the strong signals from Fe and Mn made it necessary to narrow the entrance slit in order to avoid saturating the detector.The maps were registered together using Ti (seen in both chemical-state and 10 keV maps) as a fiducial.In addition to fitting the Ce signals at the various energies of the chemical maps to read off the amounts of Ce^{3+}, Ce^{4+} and CeO_2, we also derived the total Ce amount by taking the difference between the Ce signals at 5746 eV and 5715 eV.Differencing was needed because the background from V, Ti and Ba often exceeded the signal from Ce.The upper energy was chosen because the signals from our three reference materials are equal at that energy, as shown in Fig. 1.Energy calibration was done using CeO_2 as a standard (first peak at 5730.39 eV; peak for Ce^{3+}-doped YAG at

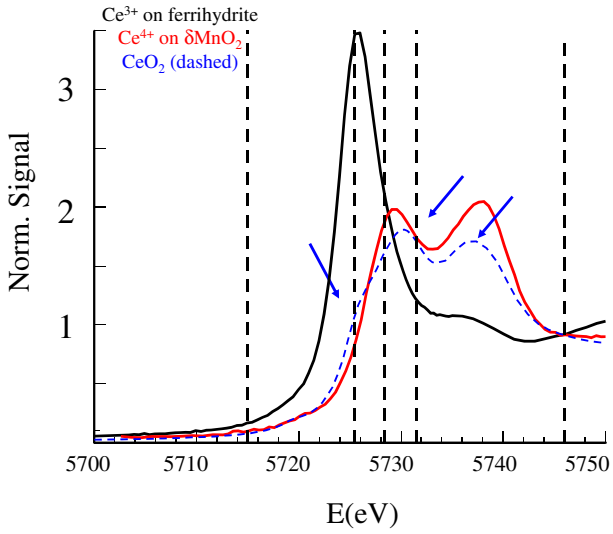

Fig. 1. XANES spectra of standards.The vertical lines show the energies used in chemical-state mapping. Arrowed features show the distinction between sorbed Ce^{4+} and CeO_2.

5725.88 eV).These maps were interpreted using as references Ce^{4+}-sorbed δ-MnO_2 (Takahashi et al., 2000), Ce-sorbed ferrihydrite and CeO_2.

The reason for using both Ce-sorbed MnO_2 and CeO_2 as Ce^{4+} references is that the XANES of CeO_2 has distinct features not found in spectra from, for instance, sorbed Ce^{4+}.Our reference spectra are shown in Fig. 1.The shoulder on the left side of the first peak and the shift of the peak positions relative to those of sorbed Ce^{4+} may be seen.The reasons for the differences between the XANES of fluorite-structure (8-coordinate) CeO_2 and other, octahedral, Ce^{4+} species have ascribed to many-body effects by (Kaindl et al., 1988; Soldatov et al., 1994). The same reference spectra were used in linear-combination fitting of spot XANES spectra from the sample.

La, Ce and Pr concentrations in Ca-rich (apatite) grains were measured by taking XRF spectra at energies of 5470 eV, 5500 eV, 5715 eV, 5746 eV, 5940 eV and 6000 eV, energies chosen to cross the L_3 edges of La, Ce and Pr.The below-edge spectra were subtracted from the above-edge spectra and then fitted using parameters derived from measurements on spectra taken on a geological fluorapatite sample (Yates Mine, Otter Lake, Ontario Canada).This sample was characterized by electron microprobe and its composition was similar to that published for a sample from the same locality (Yang et al., 2014). Cerium anomaly ratios were defined as

$$r = [Ce]/\sqrt{[La][Pr]}$$
$$\text{Anomaly} = \log\left(\frac{r}{r_{CI}}\right) \quad (1)$$

where CI refers to chondritic abundances (Anders and Grevesse, 1989).

3. Results

3.1. Cerium distribution

Figs. 2 and 3 show maps of the distribution of Ce compared with those of Mn and Fe in Inner and Outer regions of the nodule.Consistent with previous work, there are botryoidal regions of mixed Mn and Fe, displaying rhythmic oscillations of density and Ni-rich "streaks", and an Fe-rich "matrix" between botryoids (Marcus et al., 2015). The dash-